

Informing models through empirical relationships between foliar phosphorus, nitrogen and photosynthesis across diverse woody species in tropical forests of Panama

Richard J. Norby¹, Lianhong Gu¹, Ivan C. Haworth¹, Anna M. Jensen^{1,2}, Benjamin L. Turner³, Anthony P. Walker¹, Jeffrey M. Warren¹, David J. Weston⁴, Chonggang Xu⁵ and Klaus Winter³

¹Environmental Sciences Division and Climate Change Science Institute, Oak Ridge National Laboratory, Oak Ridge, TN 37830-6301, USA; ²Department of Forestry and Wood Technology, Linnaeus University, Växjö, Sweden; ³Smithsonian Tropical Research Institute, Apartado 0843-03092, Balboa, Ancon, Panama; ⁴Biosciences Division and Climate Change Science Institute, Oak Ridge National Laboratory, Oak Ridge, TN 37830-6301, USA; ⁵Earth and Environmental Science Division, Los Alamos National Laboratory, Los Alamos, NM 87545, USA

Summary

Author for correspondence:
Richard J. Norby
 Tel: +1 865 576 5261
 Email: rjn@ornl.gov

Received: 30 June 2016
 Accepted: 24 September 2016

New Phytologist (2016)
 doi: 10.1111/nph.14319

Key words: maximal Rubisco carboxylation rate (V_{cmax}), maximum electron transport rate (J_{max}), N : P ratio, nitrogen (N), phosphorus (P), photosynthesis, traits, tropical forest.

- Our objective was to analyze and summarize data describing photosynthetic parameters and foliar nutrient concentrations from tropical forests in Panama to inform model representation of phosphorus (P) limitation of tropical forest productivity.
- Gas exchange and nutrient content data were collected from 144 observations of upper canopy leaves from at least 65 species at two forest sites in Panama, differing in species composition, rainfall and soil fertility. Photosynthetic parameters were derived from analysis of assimilation rate vs internal CO₂ concentration curves (A/C_i), and relationships with foliar nitrogen (N) and P content were developed.
- The relationships between area-based photosynthetic parameters and nutrients were of similar strength for N and P and robust across diverse species and site conditions. The strongest relationship expressed maximum electron transport rate (J_{max}) as a multivariate function of both N and P, and this relationship was improved with the inclusion of independent data on wood density.
- Models that estimate photosynthesis from foliar N would be improved only modestly by including additional data on foliar P, but doing so may increase the capability of models to predict future conditions in P-limited tropical forests, especially when combined with data on edaphic conditions and other environmental drivers.

Introduction

The exchange of carbon (C) between tropical forests and the atmosphere is a dominant component of the global C cycle and a critical regulator of climate (Schimel *et al.*, 2015). Despite their importance in the global C cycle, tropical forests are not well represented in Earth system models (ESMs), in large part because of the paucity of data and conceptual understanding of tropical ecosystem process. Improving tropical models through model–data integration is an ongoing area of research (Luo *et al.*, 2011; Medlyn *et al.*, 2015; Reed *et al.*, 2015). An important objective is to include phosphorus (P) as a component of ESMs, just as the inclusion of a nitrogen (N) cycle was previously highlighted as a research priority (Thomas *et al.*, 2015). In contrast to temperate forests, the productivity of many lowland tropical forests is thought to be limited by P more than by N because they occur on old, strongly weathered soils that are depleted in P (Vitousek & Sanford, 1986; Hedin *et al.*, 2003; Lambers *et al.*, 2008). Hence, inclusion of a P cycle, and the possibility of P limitation

to productivity, should be especially important for improving the representation of tropical systems in ESMs.

A weakness of most ecosystem models is that they do not consider multiple nutrient limitations on photosynthesis, which may be especially important in tropical biomes (Dietze, 2014). Global syntheses show increased uncertainty in the relationship between maximal Rubisco carboxylation rate (V_{cmax}) and foliar N in tropical biomes, and the shallower relationship on tropical Oxisols suggests P limitation (Kattge *et al.*, 2009); model improvement is needed (Dietze, 2014). However, the specific mechanisms by which P limitation of productivity occurs remain unclear. Phosphorus is required for many compounds in plants, including those associated with metabolism (e.g. sugar phosphates, nucleic acids, nucleotides, coenzymes, phospholipids), energy transfer (triphosphonucleotides) and genetic material (i.e. nucleic acids) (Rao, 1997). Given these multiples roles, it is not surprising that many studies have demonstrated that an adequate supply of inorganic P (Pi) is essential to C assimilation, but the specific mechanisms are not nearly as clear as the direct role of N as a

constituent of the Rubisco enzyme (Ellsworth *et al.*, 2015). Orthophosphate is a primary substrate of photosynthesis, and triose phosphate is a product of photosynthesis that is exported from the chloroplast to the cytosol, but Pi is released during sucrose synthesis and recycled back to the chloroplast. Efforts to demonstrate Pi regulation of photosynthesis are confounded by internal Pi buffering mechanisms affecting the distribution of Pi between chloroplast, cytoplasm and vacuole (Rao, 1997). An inadequate supply of Pi decreases the rate of photosynthesis by limiting the capacity for ribulose 1,5 biphosphate (RuBP) regeneration, probably through effects on C supply rather than ATP supply. Effects on RuBP regeneration would most likely be manifested in J_{\max} , the maximal electron transport rate (Sivak & Walker, 1986; Domingues *et al.*, 2010). However, decreased activation of Rubisco (manifested in V_{\max}) may also be important (Rao, 1997). The tendency for homeostasis among the different processes of photosynthesis creates difficulty in disentangling possible effects of P on V_{\max} from effects of N.

There are several groups developing P models and incorporating them into ESMs (Wang *et al.*, 2010; Goll *et al.*, 2012; Yang *et al.*, 2014). The implementation of the Community Land Model that includes a P module (CLM-CNP) has been shown to improve estimates of tropical productivity (Yang *et al.*, 2014). CLM-CNP employs a supply and demand approach to determine P limitation. Supply is controlled by soil solution P through geochemical and biogeochemical processes. P limitation of productivity occurs when supply of P is less than demand, and calculation of demand is based on an independent calculation of gross primary productivity and a fixed stoichiometry. Productivity is reduced through a dimensionless coefficient that does not have an explicit physiological function. Introducing the physiological function of P into models such as CLM-CNP will be difficult mainly because of the absence of a complete conceptual model of P interaction in physiological functions, including photosynthesis. Given the absence of a clear mechanistic framework for analyzing P effects on photosynthesis, reliance on empirical relationships, such as those based on leaf N that are commonly employed to predict photosynthetic parameters (Rogers, 2014), may instead be necessary. Observations of leaf P concentration and photosynthesis (Reich & Oleksyn, 2004; Reich *et al.*, 2009; Walker *et al.*, 2014; Bahar *et al.*, 2016) can provide useful insights, whether the goal is improved conceptual representation or development of more robust empirical relations for models.

Our objective here is to assess relationships between photosynthetic parameters and foliar nutrient concentrations from the tropical forests of Panama in a manner that can inform model improvements, especially in areas where the models are weak, such as assumptions of fixed stoichiometry and absence of a direct influence of P on photosynthesis. The data were collected with a goal of capturing a wide range of species and nutrient status so as to increase the generality of our analyses. Our data will augment similar datasets (not all including P) that have been assembled from tropical forests in South America (Carswell *et al.*, 2000; Domingues *et al.*, 2007; Bahar *et al.*, 2016), West Africa (Meir *et al.*, 2007; Domingues *et al.*, 2015) and Southeast Asia (Kenzo *et al.*, 2006) with the expectation that a pan-tropical database

incorporating a wide range of edaphic, climatic and biological conditions will be most useful for model parameterization. Individual species traits are important for developing an understanding of mechanisms of response, but they are useful for large-scale models only if they can be grouped at a higher level. Many models represent the diversity of plants and their function through the use of plant functional types (PFT; Wullschleger *et al.*, 2014). All of the tree and liana species in this study were of the same PFT (tropical broadleaf evergreen). We consider whether our data support refinement of that PFT as a route toward model improvement.

Materials and Methods

Leaf gas exchange and nutrient content data were collected in January 2013 from two canopy crane sites in Panama operated by the Smithsonian Tropical Research Institute (STRI) (<http://www.stri.si.edu/english/research/facilities/terrestrial/cranes/index.php>). The Parque Natural Metropolitano (PNM) canopy crane site near Panama City (lat 8.99441°N, long -79.54330°E) is located within a lowland, semi-deciduous forest on the Pacific coast of the isthmus. This 80-yr-old forest, composed primarily of pioneer trees, receives on average 1740 mm of rain per year. The Parque Nacional San Lorenzo (SLZ) canopy crane site near Colon (lat 9.28103°N, long -79.97452°E) is in a wet evergreen forest on the Caribbean coast. This forest, which is much older and composed of late-successional, old-growth species, receives c. 3300 mm of rainfall per year. Hence, the soil at SLZ (an Oxisol) is more highly leached and nutrient deficient than the relatively fertile soil at PNM (a Mollisol). Total soil P (measured by ignition and acid extraction) at SLZ in $253 \pm 15 \text{ mg P kg}^{-1}$, compared to $446 \pm 33 \text{ mg P kg}^{-1}$ at PNM. Resin phosphate concentrations (Turner & Romero, 2009), which are assumed to more closely reflect the pool of Pi available to plants, differ much more widely between the two sites: $0.24 \text{ mg P kg}^{-1}$ at SLZ and $5.81 \text{ mg P kg}^{-1}$ at PNM. Each site has a construction crane, 42 m tall at PNM and 52 m tall at SLZ, providing access to the upper canopy of the forest over a 0.9 ha area. PNM was sampled on 22–26 January 2013 and SLZ was sampled on 29–31 January 2013 (i.e. during the early dry season).

Data for analysis of assimilation rate vs internal CO₂ concentration (A/C_i) were collected with four LI-6400XT photosynthesis units (Li-Cor Inc., Lincoln, NE, USA) from the gondola of the cranes. Fully sun-lit, mature leaves in the upper canopy of woody plants (trees and lianas) in these forests were sampled – 87 observations at PNM and 57 at SLZ – but not all of these samples remained in the final dataset, as discussed below. In addition, leaves from 17 small trees and perennial herbs in the understory were measured from ground level (5 at PNM and 12 at SLZ). Species were identified by a local botanist. The order most frequently sampled was the Rosales, followed by Malpighiales, Magnoliales and Malvalves (Supporting Information Table S1). At least 65 species and 41 families are represented in the A/C_i dataset; only two species (*Castilla elastica* in the canopy and *Dendropanax arboreus* in the understory) and eight families were common to both sites.

The A/C_i curve measurements followed the standard protocols of Long *et al.* (1996) and Long & Bernacchi (2003). The selection of ambient CO_2 concentration levels adopted the suggestion of Gu *et al.* (2010) that emphasizes the importance of points in the curved transition region of A/C_i curve for robust, unbiased parameter estimation. Exploratory light response curves were conducted to ensure that light intensities were set at saturating levels appropriate to species and their growth environments. Leaf temperatures were generally controlled to be within 3°C of the corresponding ambient air temperatures during data collection; variations in leaf temperatures were generally <2°C, and all measurements were made with limited variations in air temperature (<5°C). Relative humidity was set between 55% and 75%. Stomatal ratios were set to 1. Flow rates were mostly between 300 and 500 $\mu\text{mol s}^{-1}$. CO_2 injectors were used to control reference CO_2 in typical sequences starting from a value close to ambient (e.g. 400 ppm), decreasing to a minimum value (e.g. 50 ppm), returning to the starting value (as a check point) and then increasing to a maximum value (e.g. 1500 ppm). Each curve contained at least 10 points; most had 14–16 points (Fig. 1). The reference and sample chambers were matched manually or automatically as needed. Ample times were allowed for leaves to adapt to chamber environment and to changes in CO_2 concentrations.

When the gas exchange measurement was complete, a 373 or 423 mm^2 disk was cut from the leaf with a cork borer for determination of specific leaf area (SLA) and the remaining leaf was preserved for nutrient analysis. Leaf disks and whole leaves were placed in a 70°C forced draft oven on the day of collection, dried for 2 d, leaf disks were weighed, and whole leaves were ground. Total carbon (C) and N concentrations were determined by dry combustion on a Thermo Flash 1112 Elemental Analyzer

(Waltham, MA, USA). Total P was determined by dry ashing at 550°C for 4 h, the ash dissolved in 1 M HCl (Karla, 1998) and P concentrations determined by automated molybdate colorimetry on a Lachat Quikchem 8500 (Hach Ltd, Loveland, CO, USA). Certified reference samples (NIST 1515, apple leaves; NIST 1547, peach leaves) and internal laboratory control standards were included in all analyses. Results for NIST standards were within 3% of the certified values.

The measured A/C_i curves were analyzed with the approach of Gu *et al.* (2010) as implemented in LeafWeb (<http://www.leafweb.org>). This approach avoids pre-assigning transition thresholds and therefore limitation states by enumerating all possible limitation state combinations for a given A/C_i curve. The scheme of enumeration considers that instead of occurring in a random sequence, the three limitation states must follow a certain pattern along the C_i axis in order to be consistent with the FvCB model (Farquhar *et al.*, 1980); i.e., the C_i values for the Rubisco-limited state should be smaller than those of the RuBP regeneration-limited state, which in turn should be smaller than for the TPU-limited points. Each limitation scenario with the limitation state of each point fixed is then fit separately to ensure a smooth cost function for the change-point FvCB model. During this process, inadmissible fits (parameter estimates that produce a limitation state other than those assigned) are detected and penalized. The best fit among all scenarios is selected. Thus, the approach of Gu *et al.* (2010) has two nested optimizations – the optimization for limitation state combination and the optimization for parameters from the optimized limitation state combination. The TPU-limited region of the curve is described by

$$A = \frac{3V_{\text{TPU}}(C_i - \Gamma^*)}{C_i - (1 + 3\alpha)\Gamma^*} - R_d \quad \text{Eqn 1}$$

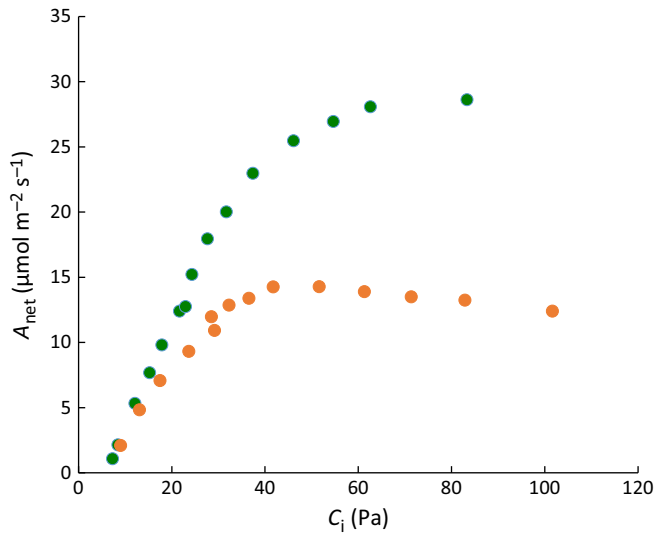


Fig. 1 CO_2 assimilation rate (A_{net}) vs internal CO_2 concentration (C_i) curves of two trees differing in foliar nutrient status. Green (upper) curve is from *Cordia alliodora* (Boraginaceae). Area-based phosphorus content (P_{area}) = 0.147 g m^{-2} , nitrogen content (N_{area}) = 3.58 g m^{-2} and maximal Rubisco carboxylation rate (V_{cmax}) = 65.2 $\mu\text{mol m}^{-2} \text{s}^{-1}$. Red (lower) curve is from *Crescentia cujete* (Bignoniaceae). P_{area} = 0.092 g m^{-2} , N_{area} = 1.18 g m^{-2} and V_{cmax} = 26.2 $\mu\text{mol m}^{-2} \text{s}^{-1}$.

(Γ^* , CO_2 compensation point; V_{TPU} , rate of triose phosphate export from the chloroplast (also referred to as T_p); α , nonreturned fraction of the glycolate carbon recycled in the photorespiratory cycle; R_d , mitochondrial (day) respiration). A decline in A at high C_i is characterized by the parameter α , with a steeper decline corresponding to a larger α . α is understood as being linked with the release of phosphate from photosynthetic biochemical cycles to the cytosol (von Caemmerer, 2000). Parameters were standardized to a reference temperature of 25°C. The kinetic constants and coefficients in the temperature response functions, taken from Table 1 of Sharkey *et al.* (2007), were kept the same for all A/C_i curves. The temperature correction does not account for the likelihood of these tropical species having higher temperature optima than those established for temperate and boreal species, but insufficient data are available for establishing robust temperature response functions exclusively for tropical species.

A/C_i data were inspected and curves that had discontinuities or fewer than 10 points were omitted. The final dataset included 105 observations with one or more photosynthetic parameter from 48 identified species and 13 plants that could not be

identified to genus. The A/C_i data were merged with nutrient content data, which included 144 observations (39 entries with nutrient data had no corresponding photosynthetic parameters). The dataset is publically available (Gu *et al.*, 2016). Values of wood density for 45 species in this dataset were gathered from the Global Wood Density Database (Chave *et al.*, 2009; Zanne *et al.*, 2009) and from Wright *et al.* (2010). No measurements of wood density were made on the individual trees sampled in this study; hence, for this *post hoc* analysis we relied necessarily on the established database. Mean values of photosynthetic parameters and foliar nutrient content were compared across sites and by taxonomic order. Statistical analyses were done using STATISTIX 8 (Analytical Software, Tallahassee, FL, USA). Natural logs of V_{cmax} , J_{max} and V_{TPU} of canopy leaves (standardized to 25°C) were regressed against natural logs of foliar N and P contents per unit leaf area (N_{area} and P_{area}). These relationships were assumed to be asymmetric (i.e., dependent and independent variables are not switchable; Smith, 2009) and ordinary least squares (OLS) regressions were used. Relationships between V_{cmax} and J_{max} , V_{TPU} and J_{max} , and N_{area} and P_{area} were assumed to be symmetrical, so reduced major axis regression (RMA) was used with one-delete jack-knife estimates of regression coefficients and r^2 and the associated standard errors (Bohonak, 2004). Multivariate regression analysis of J_{max} and V_{cmax} against natural logs of N_{area} , P_{area} , N_{mass} , P_{mass} , SLA, and for a subset of species, wood density, was conducted with a requirement of a statistical power of $P < 0.05$ for a variable to enter the model; the best regression was chosen based on smallest value of Akaike's information criterion (AIC).

Results

The plants sampled in these communities exhibited a wide range of nutrient status (Fig. 2). Foliar N concentrations were between 13 and 50 mg g⁻¹, whereas foliar P concentrations were between 0.5 and 3.1 mg g⁻¹. Mean N and P concentrations were less at SLZ than at PNM (Table 1), reflecting the known difference in soil nutrient status (Condit *et al.*, 2013). Leaves in the heavily shaded understory contained similar nutrient concentrations on a mass basis compared to canopy leaves, but because SLA was

considerably greater in the understory, their area-based nutrient contents were much less than those of canopy leaves. The N : P ratio was greater at SLZ (Table 1), supporting our assumption that P limitation is more important at that site. This was expected based on resin phosphate concentrations (0.24 mg P kg⁻¹ at SLZ and 5.81 mg P kg⁻¹ at PNM) and soil classes (Oxisols at SLZ, Mollisols at PNM). Increasing values of N : P ratio were associated more with declining P_{mass} than with increasing N_{mass} . The one canopy species common to both sites in this dataset (*Castilla elastica*) showed similar patterns as the site means. Taking an N : P ratio > 20 as a rough indication of P limitation (Güsewell, 2004), 57% of the observations at SLZ indicated P limitation compared to 28% of the observations at PNM (Fig. 2). Few observations indicated N limitation (N : P < 10), but many observations were indicative of co-limitation (10 $<$ N : P $<$ 20; Güsewell, 2004).

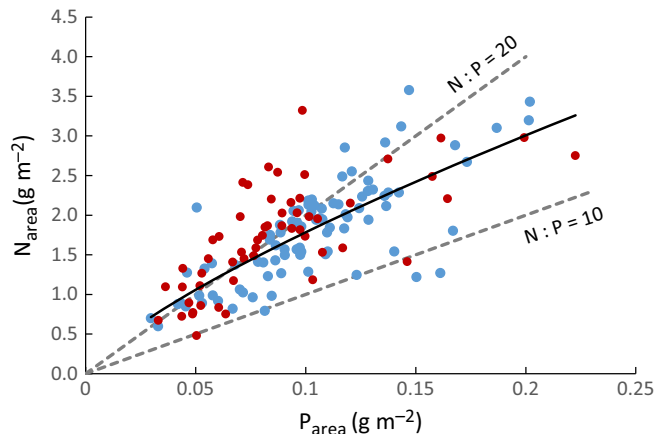


Fig. 2 Relationship between area-based nitrogen and phosphorus content (N_{area} and P_{area}) of canopy leaves by site. Blue symbols, Parque Natural Metropolitano (PNM); red symbols, Parque Nacional San Lorenzo (SLZ), with reduced major axis regression line through all points (Table 3). Dashed lines represent N : P mass ratios of 10 and 20, which are roughly indicative of P limitation (points above the N : P 20 line), N limitation (points below the N : P 10 line) or co-limitation for points between the lines.

Table 1 Foliar nutrient characteristics and specific leaf area of canopy and understory trees sampled at Parque Natural Metropolitano and Parque Nacional San Lorenzo canopy crane sites in Panama

	Upper canopy		Understory
	PNM (<i>n</i> = 82)	SLZ (<i>n</i> = 44)	PNM and SLZ (<i>n</i> = 17)
P_{mass} (mg g ⁻¹)	1.54 ± 0.06 (0.71–3.07)	1.08 ± 0.07 (0.53–2.78)	1.38 ± 0.09 (0.98–2.20)
P_{area} (g m ⁻²)	0.106 ± 0.004 (0.033–0.202)	0.097 ± 0.006 (0.036–0.223)	0.050 ± 0.002 (0.030–0.067)
N_{mass} (mg g ⁻¹)	25.81 ± 0.78 (13.50–49.80)	21.543 ± 0.82 (13.80–40.30)	26.49 ± 2.34 (11.60–45.20)
N_{area} (g m ⁻²)	1.83 ± 0.07 (0.60–3.58)	1.95 ± 0.08 (0.84–3.32)	0.97 ± 0.09 (0.48–2.09)
N : P	17.55 ± 0.41 (7.87–27.64)	21.563 ± 0.91 (9.68–33.77)	19.51 ± 1.70 (9.53–41.41)
SLA (cm ² g ⁻¹)	155.2 ± 6.8 (78.0–355.2)	122.5 ± 6.5 (64.4–283.7)	278.4 ± 16.9 (154.2–418.5)

Data are means \pm SE with the range given in parentheses. PNM, Parque Natural Metropolitano; SLZ, Parque Nacional San Lorenzo; P_{mass} and N_{mass} , mass-based nitrogen and phosphorus contents of leaves; P_{area} and N_{area} , area-based phosphorus and nitrogen contents of leaves; N : P, nitrogen-to-phosphorus mass ratio; SLA, specific leaf area.

Photosynthetic parameters also varied over a wide range (Table 2). A_{\max} (the CO₂ assimilation rate at saturating CO₂ and light) of upper canopy leaves was 10% greater at PNM, consistent with the greater nutrient concentrations at that site (Table 1), and photosynthetic N use efficiency (NUE, calculated as A_{\max} divided by N_{area}) was 18% greater at PNM (Table 2). There was no difference between sites in P use efficiency (PUE, Table 2) and no effect of P_{area} on NUE (not shown). V_{cmax} in *Castilla elastica* was $44.1 \pm 1.2 \mu\text{mol m}^{-2} \text{s}^{-1}$ at PNM ($n=2$) and $28.6 \pm 1.9 \mu\text{mol m}^{-2} \text{s}^{-1}$ ($n=2$) at SLZ, significantly different by Student's *t*-test ($P<0.02$). Generally, however, site differences are confounded with species differences and cannot easily be evaluated. At a higher taxonomic level, there are five plant orders with at least three species in our data base. There was wide variation among species within order in V_{cmax} (Fig. 3a), N:P ratio (Fig. 3b), or other photosynthetic or nutrient parameters, but no significant differences among these orders. We also saw no difference in these parameters between trees and lianas (Fig. 3a,b). Within the Genitiales, Magnoliales and Rosales, differences in V_{cmax} between sites (not shown) were similar to the overall difference between sites (Table 2), suggesting that site differences are more important than phylogenetic differences.

Two contrasting A/C_i curves are shown in Fig. 1, both from PNM. The curve for *Cordia alliodora* (family Boraginaceae) exhibits a saturating response, typical of A/C_i curves most commonly reported. The curve for *Cinnamomum triplinerve* (family Lauraceae), which has lower foliar N and P concentrations, exhibits a declining A at high C_i. Declining A at high C_i, characterized by the parameter α in Eqn 1, is generally thought to be indicative of feedback inhibition through TPU (Long & Bernacchi, 2003) or limitation of Pi recycling by photorespiratory activity (Diaz-Espejo *et al.*, 2006; Ellsworth *et al.*, 2015). Because α is assumed to be the fraction of the glycolate carbon not returned to the chloroplast, it should take a value between 0 (a flat line) and 1 (the steepest possible decline). Seventy-two observations had calculated α values greater than 0. Among these observations, 27 had values >1, suggesting the biochemical meaning of this parameter may be uncertain and require re-examination. V_{cmax}

and J_{max} were well correlated ($r^2=0.87$; Fig. 4a), as were V_{TPU} and J_{max} ($r^2=0.95$; Fig. 4b). All three photosynthetic parameters showed significant relationships with foliar P and N status; area-based relationships as shown in Fig. 5 were generally stronger than mass-based relationships. In all cases power functions were stronger than simple linear relationships. There were no significant differences between site-specific regressions. Four species were measured with at least four replicate trees; the relationship between V_{cmax} and P_{area} within species was similar to the relationship across species (Fig. S1). Observations from understory plants were not included in any of these regressions, but they generally fell within the same distribution.

Using multivariate regression, the best expression of photosynthetic traits expressed J_{max} as functions of both N and P (Table 3). Coefficients of both terms were statistically significant (N_{area}, $P<0.001$; P_{area}, $P<0.015$) and AIC was reduced relative to that of the regression based on just N_{area}, but the strength of the relationship increased only modestly over that based on N content alone (r^2 increased from 0.49 to 0.54; Table 3). The empirical equations for J_{max} and V_{cmax} (Table 3) were tested against the completely independent data from Peru of Bahar *et al.* (2016). The modeled values matched the mean values of the data well (within 2% for J_{max} ($n=183$) and 14% for V_{cmax} ($n=241$) and explained 14% of the variation in J_{max} and 11% of the variation in V_{cmax} ($n=241$) (Fig. S2a,b). Predictions of plot-level values, which are closer to the relevant scale for modeling, were better, with 43–46% of variation explained by our empirical equations (Fig. S2c,d). The relationships between V_{cmax} and either N_{area} or P_{area} were not improved by including both terms. Wood density, which correlates with growth rate, successional status and other traits (Nascimento *et al.*, 2005; Chave *et al.*, 2009; Wright *et al.*, 2010), was a significant predictor of J_{max} (Fig. 4c), strengthening the relationship with N and P for a subset of plants for which wood density data were available. With wood density included, 69% of the variation in J_{max} could be explained (Table 3). Wood density did not differ significantly between the two sites (0.55 g cm^{-3} at PNM and 0.49 g cm^{-3} at SLZ). We explored possible correlations with other leaf traits available for some of the species in our dataset, including leaf

Table 2 Photosynthetic parameters of canopy and understory plants sampled at Parque Natural Metropolitano and Parque Nacional San Lorenzo canopy crane sites in Panama

	Upper canopy		Understory
	PNM ($n=64$)	SLZ ($n=30$)	PNM and SLZ ($n=11$)
V _{cmax,25} ($\mu\text{mol m}^{-2} \text{s}^{-1}$)	45.53 ± 1.91 (16.29–77.21)	39.88 ± 2.77 (15.21–76.32)	27.40 ± 3.04 (13.83–40.23)
J _{max,25} ($\mu\text{mol m}^{-2} \text{s}^{-1}$)	71.42 ± 2.87 (27.58–125.31)	71.06 ± 4.26 (30.97–116.51)	45.18 ± 3.46 (26.09–65.45)
V _{TPU,25} ($\mu\text{mol m}^{-2} \text{s}^{-1}$)	4.93 ± 0.18 (2.02–8.35)	4.67 ± 0.27 (2.48–7.55)	3.20 ± 0.21 (1.90–4.48)
A _{max} ($\mu\text{mol m}^{-2} \text{s}^{-1}$)	17.06 ± 0.76 (6.47–32.92)	15.52 ± 0.87 (7.80–25.62)	9.77 ± 0.72 (5.64–14.01)
PUE ($\mu\text{mol CO}_2 \text{ mol}^{-1} \text{ P s}^{-1}$)	5294 ± 226 (1534–11262)	5386 ± 333 (2775–9857)	6495 ± 519 (3921–9239)
NUE ($\mu\text{mol CO}_2 \text{ mol}^{-1} \text{ N s}^{-1}$)	136 ± 7 (38.97–323.01)	115 ± 7 (45.54–210.17)	172 ± 12 (89.39–218.19)

Data are means \pm SE with the range given in parentheses. PNM, Parque Natural Metropolitano; SLZ, Parque Nacional San Lorenzo; V_{cmax,25}, maximal Rubisco carboxylation rate, standardized to 25°C; J_{max,25}, maximum electron transport rate, standardized to 25°C; V_{TPU,25}, the rate of triose phosphate export from the chloroplast, standardized to 25°C; A_{max}, CO₂ assimilation rate at saturating light and CO₂; PUE, photosynthetic phosphorus use efficiency; NUE, photosynthetic nitrogen use efficiency.

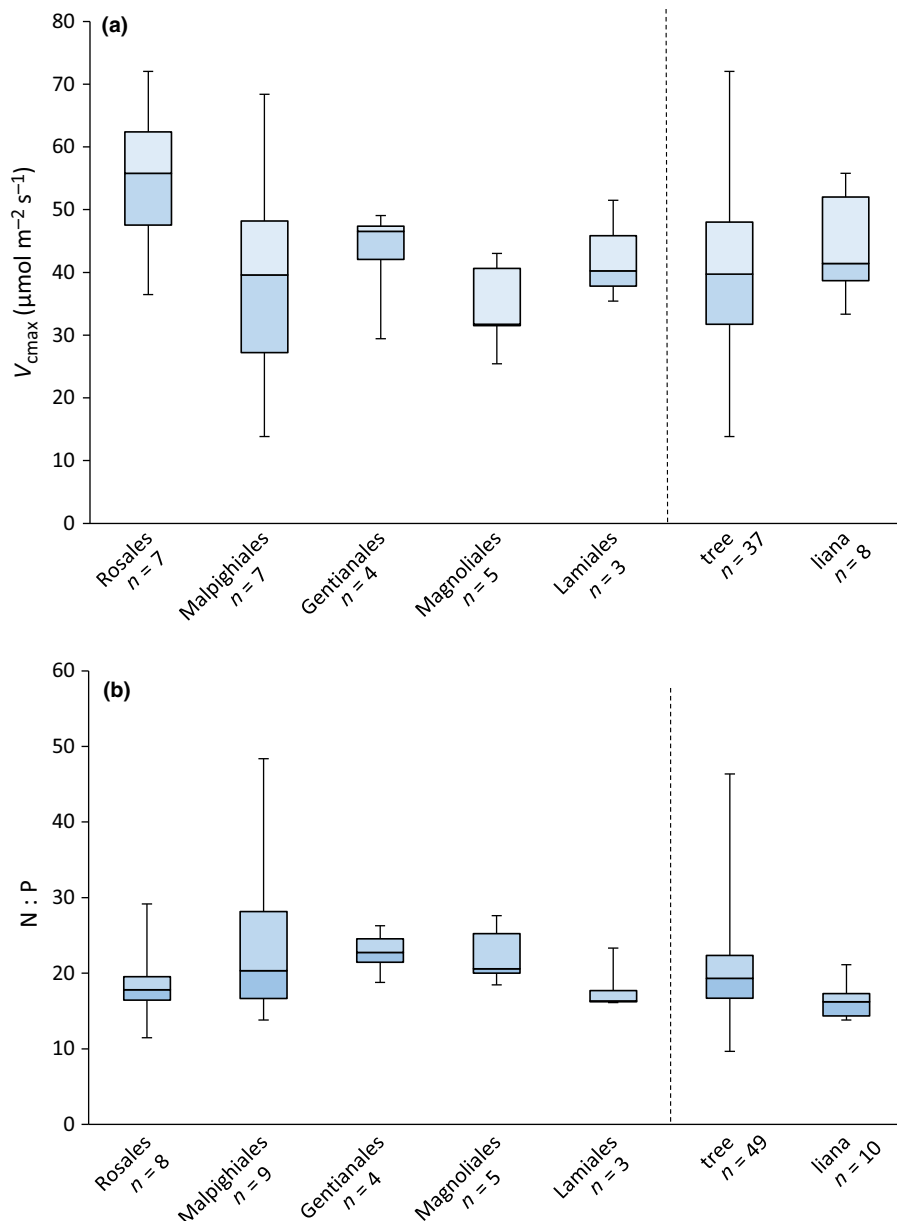


Fig. 3 Box plots of (a) maximal Rubisco carboxylation rate ($V_{c\text{max}}$) and (b) nitrogen-to-phosphorus mass ratio (N : P) by taxonomic order for those orders with at least three species in the dataset, and a comparison of trees and lianas. The bottom of the darker blue box indicates the 25th percentile of the data, the top of the lighter blue box indicates the top the 75th percentile and the horizontal line within the box is the median value. The whiskers correspond to the minimum and maximum of the data ranges. Multiple observations within a species were averaged. No differences between orders or growth form are statistically significant.

dimensions, organic and mineral contents, and P and N affinities (Condit *et al.*, 2013), but none were especially informative.

Discussion

The range of foliar P concentrations observed here (0.5–3.0 mg g⁻¹) mostly covers the range reported for other tropical forests: 0.4–1.2 mg g⁻¹ in French Guiana (Hättenschwiler *et al.*, 2008); 0.7–1.1 mg g⁻¹, 0.24–4.09 mg g⁻¹, 0.5–2.0 mg g⁻¹ and 0.42–1.35 mg g⁻¹ in different studies in the Amazon basin (Fyllas *et al.*, 2009; Mercado *et al.*, 2011; Domingues *et al.*, 2015; Bahar *et al.*, 2016); 0.9–1.0 mg g⁻¹ and 1.1–1.4 mg g⁻¹ in West Africa (Meir *et al.*, 2007; Domingues *et al.*, 2015); and 0.9 mg g⁻¹ across the tropics overall (Reich *et al.*, 2009). However, the mean values we report for these two forests in Panama,

1.1 mg g⁻¹ (SLZ) and 1.5 mg g⁻¹ (PNM), are somewhat higher than means reported elsewhere, possibly reflecting greater site fertility but confounded by different species composition across sites. The N : P ratios reported here (17.6 at PNM and 21.5 at SLZ) are also comparable with values for other tropical forests: 18.8 (Reich *et al.*, 2009), 10–40 across different sites in the Amazon (Mercado *et al.*, 2011) and 15–30 in lowland forests of Peru (Bahar *et al.*, 2016). Santiago *et al.* (2005) measured leaf and litter chemistry on eight species at each of these same sites in Panama. The mean P concentration was similar at PNM (1.4 vs 1.5 mg g⁻¹), but was lower at SLZ than we report (0.76 vs 1.1 mg g⁻¹). However, the P concentrations in our data for the six species in common with Santiago's dataset were closer: 0.96 mg g⁻¹. This comparison emphasizes the importance of species identity in determining the community-level nutritional status of a site.

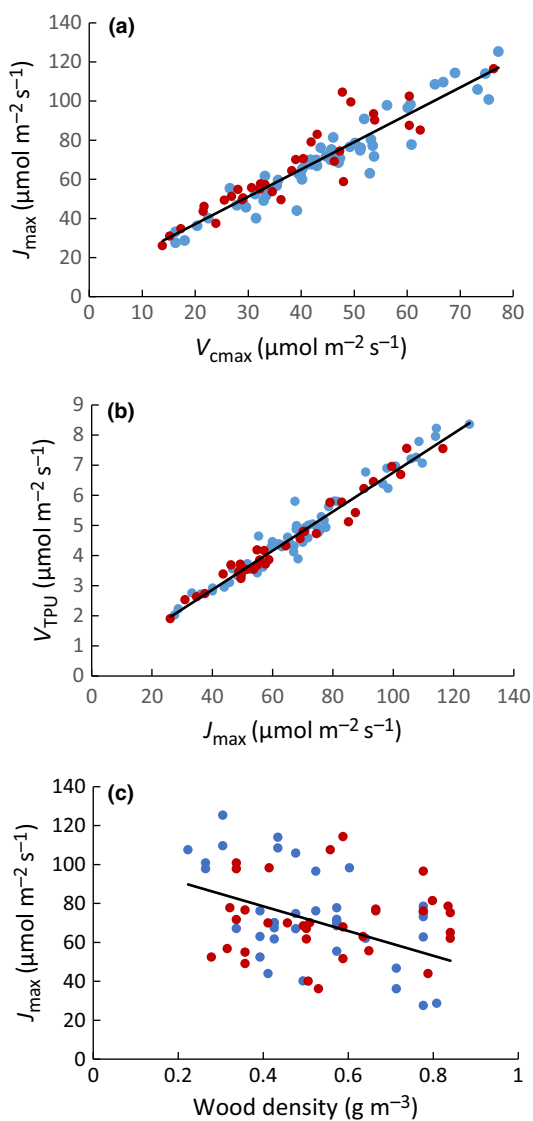


Fig. 4 Relationships between photosynthetic parameters and wood density, by site. Blue symbols, Parque Natural Metropolitano (PNM); red symbols, Parque Nacional San Lorenzo (SLZ). Photosynthetic parameters are maximal Rubisco carboxylation rate (V_{cmax}), maximum electron transport rate (J_{max}) and the rate of triose phosphate export from the chloroplast (V_{TPU}), all standardized to 25°C . (a) $J_{\text{max}} = 1.48 \times V_{\text{cmax}} + 6.30$, $r^2 = 0.87$; (b) $V_{\text{TPU}} = 0.06 \times J_{\text{max}} + 0.15$, $r^2 = 0.95$; (c) $J_{\text{max}} = -63.0 \times \text{wood density} + 107.0$, $r^2 = 0.21$. See Table 3 for full statistical information. Wood density values came from Chave *et al.* (2009) and Wright *et al.* (2010) and were not measured on the same individuals used in this study.

Photosynthetic parameters measured here are consistent with values reported from other tropical forest sites. V_{cmax} (average $40\text{--}46 \mu\text{mol m}^{-2} \text{s}^{-1}$ at the two sites) compared to $39\text{--}46 \mu\text{mol m}^{-2} \text{s}^{-1}$ across three sites in Cameroon (Domingues *et al.*, 2015), $49\text{--}79 \mu\text{mol m}^{-2} \text{s}^{-1}$ (with an additional value of 124) in a different study in Cameroon (Meir *et al.*, 2007); $43\text{--}52 \mu\text{mol m}^{-2} \text{s}^{-1}$ in the Brazilian Amazon (Carswell *et al.*, 2000; Domingues *et al.*, 2007); and $26\text{--}79 \mu\text{mol m}^{-2}$ across 18 lowland sites in Peru (Bahar *et al.*, 2016). Our values for J_{max} , however, average less than those reported in most of these other

studies and the slope (1.47) of the $J_{\text{max}} : V_{\text{cmax}}$ relationship (Fig. 4a) is less than those from global analyses (1.64 in Wullschleger, 1993; 1.67 in Medlyn *et al.*, 2002), but within the range reported for dipterocarp species in Malaysia (1.37–1.77, Kenzo *et al.*, 2006) and lowland forest trees in Peru (1.34, Bahar *et al.*, 2016). Rogers (2014) reported that most ESMs use a value for V_{cmax} for tropical broadleaf evergreen trees of $18\text{--}60 \mu\text{mol m}^{-2} \text{s}^{-1}$, which is broadly compatible with our data and other published data for forests dominated by this plant functional type (PFT). The Community Land Model (CLM) v4.5 sets V_{cmax} for the PFT at $41 \mu\text{mol m}^{-2} \text{s}^{-1}$ (Oleson & Lawrence, 2013), which is very close to our values. J_{max} is set at $1.97 \times V_{\text{cmax}}$, or $80.8 \mu\text{mol m}^{-2} \text{s}^{-1}$ for the PFT, and V_{TPU} at $0.167 \times V_{\text{cmax}}$, or $6.85 \mu\text{mol m}^{-2} \text{s}^{-1}$; both of these values are greater than our measured values (Table 2).

Although there is wide variation in the measured photosynthetic and nutrient traits across the species studied here, we note that all of the species are of the same PFT and are treated the same in models. Is there a basis for providing a finer resolution of PFTs in models? Models that are to be applied regionally or globally certainly cannot incorporate all species, and this is particularly true for the tropics, where plant diversity is very high. Furthermore, the models operate at spatial scales that must take an average value of traits across many individuals and in the tropics, that will mean across many different species (or even families and orders) within the same PFT. Townsend *et al.* (2007), noting the wide range in N:P ratio at a given site, concluded that species identity and their life history strategies and physiological capabilities are the dominant controls on N:P in the tropics. Likewise, Garrish *et al.* (2010) observed that *Ficus insipida* maintained its foliar N:P against a wide variation in N:P in the substrate, suggesting that species foliar N:P may be relatively well-constrained. However, we saw no basis for grouping the individual species in this dataset to create a finer-scale PFT based on phylogeny or growth form (trees vs lianas). Nevertheless, there were clear differences between the two sites that could be represented in models if there were a way to predict that difference. Making a connection between foliar element concentrations and site fertility has long been an objective in ecosystem ecology, but the high variability of N:P ratios in tropical trees makes this approach challenging (Townsend *et al.*, 2007). The site differences reflect differences in community composition, which probably cannot be recreated in a model, but community composition reflects adaptations to soil fertility and climate (Condit *et al.*, 2013), which can be represented in a model. Hence, the best approach may be to allow flexibility in traits based on soil or climatic drivers rather than prescribing trait values for a PFT or sub-PFT group. With only two sites in this study, we cannot evaluate quantitatively the influence of site fertility on photosynthetic parameters, but across 18 sites in Peru differing widely in soil conditions, total soil P was a significant predictor (along with foliar P_{area}) of V_{cmax} (Bahar *et al.*, 2016). However, the empirical equations for V_{cmax} and J_{max} developed by Bahar *et al.* (2016) fail to capture the observed variability in our Panama dataset, although they do adequately reproduce the mean values of the two plots (Fig. 6a,b). Because studies such as

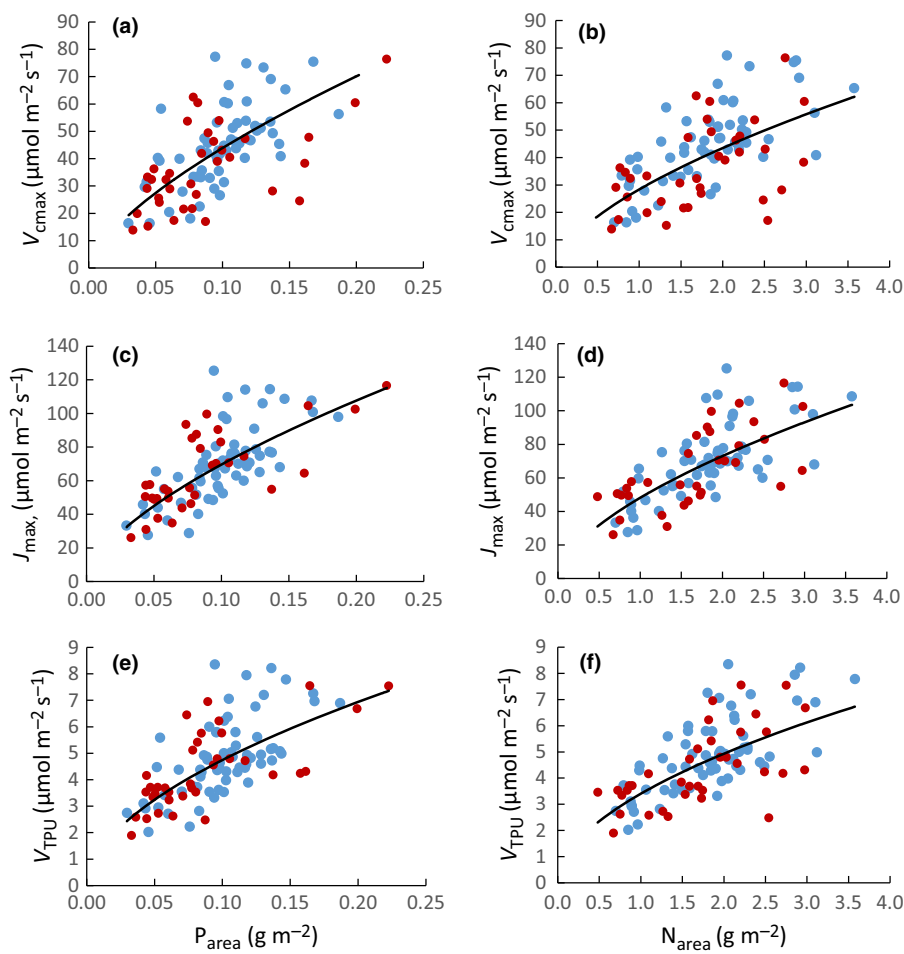


Fig. 5 Relationships between photosynthetic parameters (standardized to 25°C) of canopy woody plants (trees and lianas) and (a, c, e) area-based foliar phosphorus content (P_{area}) and (b, d, f) area-based nitrogen content (N_{area}) at Parque Natural Metropolitano (PNM, blue) and Parque Nacional San Lorenzo (SLZ, red). The photosynthetic parameters are (a, b) maximal Rubisco carboxylation rate (V_{cmax}), (c, d) maximum electron transport rate (J_{max}) and (e, f) the rate of triose phosphate export from the chloroplast (V_{TPU}). See Table 3 for regression statistics.

these are combined into a pan-tropical analysis, global datasets describing soil P (Yang *et al.*, 2013) will be an especially valuable resource for modeling.

We found significant bivariate relationships between V_{cmax} , J_{max} and V_{TPU} , and either N_{area} or P_{area} . Bahar *et al.* (2016) also reported significant relationships between V_{cmax} or J_{max} and foliar N and P, but the relationships explained very little of the overall variation ($r^2 < 0.05$). Rowland *et al.* (2015) did not see any significant relationships at the Caxiuanã site in the Amazon. In contrast to the significant role of total soil P in predicting photosynthetic capacity in Peru (Bahar *et al.*, 2016), none of the relationships between photosynthetic parameters and P_{area} differed between our two sites in Panama despite the difference in site fertility. However, from a modeling perspective, it is advantageous if site-specific relationships are not required for predicting the photosynthetic parameters. Few studies have reported relationships with V_{TPU} . Ellsworth *et al.* (2015) concluded that V_{TPU} can be limiting at high C_i in a wide range of species across P gradients, and P limitation to photosynthetic capacity is probably more common than previously thought.

The improvement in predictions of photosynthesis when wood density was included suggests that a modeling approach which incorporates trait covariation could be useful. The relationship between J_{max} and wood density is unlikely to be a direct cause-

and-effect relationship but, rather, a reflection of a trait economics spectrum that includes an association between dense wood, a lower fraction of conduits, and lower rates of transpiration and photosynthesis (Patiño *et al.*, 2009). There are many observations of a negative relationship between stand-level wood density and soil fertility (e.g. Quesada *et al.*, 2012), which largely reflects differences in species composition, but we saw no significant difference in wood density of our two sites. We recognize that wood density of a given species can in some circumstances vary with soils or climate (as discussed by Patiño *et al.*, 2009 and Quesada *et al.*, 2012), which could compromise our use of data from other studies, although generally wood density is highly conserved phylogenetically (Chave *et al.*, 2006). A survey of 325 species on Barro Colorado Island in Panama indicated that within-species variation in wood density was an order of magnitude lower than among-species variation (Hietz *et al.*, 2016). A more robust analysis should emerge in future studies by measuring wood density of the same individuals used in the A/C_i analysis. This could establish a stronger foundation and perhaps a mechanistic basis for using the Global Wood Density Database as a key source for trait covariation modeling approaches.

The distribution of foliar N:P ratios in our dataset (Fig. 2) suggests that many of the trees which we measured were co-limited by N and P. However, N:P ratios are not definitive of N

Table 3 Statistical summary or regressions shown in Figs 2, 4, 5 and 6

Relationship	Regression type	Constant ± SE	Coefficient ± SE	F	n	r^2
$\text{Log}_e(V_{\text{cmax}})$ vs $\text{Log}_e(P_{\text{area}})$	OLS	5.16 ± 0.22	0.62 ± 0.09	43.15	85	0.34
$\text{Log}_e(V_{\text{cmax}})$ vs $\text{Log}_e(N_{\text{area}})$	OLS	3.34 ± 0.07	0.61 ± 0.10	36.54	85	0.31
$\text{Log}_e(J_{\text{max}})$ vs $\text{Log}_e(P_{\text{area}})$	OLS	5.72 ± 0.18	0.64 ± 0.08	71.31	83	0.47
$\text{Log}_e(J_{\text{max}})$ vs $\text{Log}_e(N_{\text{area}})$	OLS	3.82 ± 0.05	0.67 ± 0.08	76.58	83	0.49
$\text{Log}_e(V_{\text{TPU}})$ vs $\text{Log}_e(P_{\text{area}})$	OLS	2.85 ± 0.17	0.56 ± 0.07	64.45	88	0.43
$\text{Log}_e(V_{\text{TPU}})$ vs $\text{Log}_e(N_{\text{area}})$	OLS	1.18 ± 0.05	0.60 ± 0.08	63.86	88	0.43
$\text{Log}_e(N_{\text{area}})$ vs $\text{Log}_e(P_{\text{area}})$	RMA	2.81 ± 0.13	0.96 ± 0.06	124.7	127	0.50
J_{max} vs V_{cmax}	RMA	6.30 ± 2.49	1.47 ± 0.06	535.1	80	0.87
V_{TPU} vs J_{max}	RMA	0.15 ± 0.10	0.066 ± 0.001	1556.2	83	0.95
J_{max} vs wood density	OLS	109.8 ± 8.9	-70.3 ± 16.4	18.46	54	0.26
Walker V_{cmax} vs measured V_{cmax}	RMA	22.36 ± 2.18	0.574 ± 0.053	38.90	85	0.32
Walker J_{max} vs measured J_{max}	RMA	32.24 ± 5.03	0.757 ± 0.081	61.09	80	0.43
LUNA V_{cmax} vs measured V_{cmax}	RMA	23.08 ± 2.70	0.698 ± 0.064	36.82	82	0.31
LUNA J_{max} vs measured J_{max}	RMA	26.41 ± 6.20	1.037 ± 0.098	56.84	80	0.42
$\text{Log}_e(J_{\text{max}})$ vs $\text{Log}_e(N_{\text{area}})$, $\text{Log}_e(P_{\text{area}})$	SMLR	4.77 ± 0.32	$\text{Log}_e(N_{\text{area}}): 0.40 \pm 0.12$ $\text{Log}_e(P_{\text{area}}): 0.34 \pm 0.11$	46.35	83	0.54
$\text{Log}_e(J_{\text{max}})$ vs $\text{Log}_e(N_{\text{area}})$, $\text{Log}_e(P_{\text{area}})$, wood density	SMLR	4.60 ± 0.34	$\text{Log}_e(N_{\text{area}}): 0.62 \pm 0.13$ $\text{Log}_e(P_{\text{area}}): 0.23 \pm 0.12$ Density: -0.35 ± 0.18	39.98	61	0.69

Regression type: OLS, ordinary least squares; RMA, reduced major axis; SMLR, stepwise multiple linear regression. F statistics for RMA regressions were generated from the equivalent OLS regression. All regressions are significant at $P < 0.0001$. V_{cmax} , maximal Rubisco carboxylation rate, standardized to 25°C; J_{max} , maximum electron transport rate, standardized to 25°C; V_{TPU} , the rate of triose phosphate export from the chloroplast, standardized to 25°C; P_{area} and N_{area} , area-based phosphorus and nitrogen contents of leaves. Walker refers to the empirical relationship described by Walker *et al.* (2014); LUNA refers to the model in Xu *et al.* (2012) and Ali *et al.* (2016).

or P limitation, and the analysis does not suggest any mechanism for co-limitation. Analysis of similar datasets by Domingues *et al.* (2010) and Mercado *et al.* (2011) provided evidence and a mechanistic basis for co-limitation of photosynthesis by N and P in tropical trees. In some of their plants, both J_{max} and V_{cmax} were limited by P, and in other plants both were limited by N, but in many plants J_{max} was limited by P whereas V_{cmax} was limited by N. This result is consistent with the recognition of the large N demand for Rubisco, which is reflected in V_{cmax} , and the many transformations of P-rich molecules involved in ribulose 1,5 biphosphate (RuBP) regeneration, which is reflected in J_{max} (Domingues *et al.*, 2010). We attempted a similar analysis, using both the quasi-Newton optimization algorithm used by Domingues *et al.* (2010) (the ‘BFGS’ method of the ‘OPTIM’ function in R; R Core Development Team, 2011), as well as the generalized simulated annealing algorithm (the ‘GENSA’ function in R) that in testing was found to consistently converge to true parameter values. However, the fitted parameters of the Domingues *et al.* (2010) function were highly sensitive to the dataset used during the parameter optimization. Inclusion or removal of a small number of data points changed parameter estimates to the extent of switching whether J_{max} or V_{cmax} was primarily limited by N or P. Hence, we do not have confidence in the analysis when applied to our dataset, and we recommend that parameter confidence intervals be estimated with bootstrapping or Bayesian methods in future use of the analysis.

Many models have V_{cmax} as an input parameter to drive photosynthesis and gross primary production (Rogers, 2014). Some P-enabled models (e.g. CLM-CNP; Yang *et al.*, 2014) use a single invariant value of foliar C:P ratio as input for calculating P

demand and P limitation for a given PFT. All of the woody plants in this study – including long-lived and slow-growing canopy trees, fast-growing pioneer species, palms and lianas – were of a single PFT, broadleaf evergreen tropical. Foliar C:P ratio is set at 600 (or 0.8 mg P g⁻¹ leaf dry mass) across all species and site conditions (X. Yang, pers. comm.). Although the overall mean of nutrient concentrations and photosynthetic parameters from our study were consistent with what many models use, perhaps models could be improved if that broad PFT definition were subdivided into groups with different values of P_{area} or V_{cmax} . However, we saw no basis in this dataset to separate the observations by taxonomic or phylogenetic status, and the relationship between V_{cmax} and P_{area} (and similar relationships) was independent of species. Although there were differences between the two sites, reflecting site differences in fertility, data from both sites could be explained by the same relationships despite the almost complete absence of any common species. A model that could estimate foliar nutritional status from soil characteristics might be able to capture the difference in photosynthesis between sites without any specific knowledge of species composition.

In order to explore the implications of our Panama data to global modeling, we compared our data against the empirical relationships between V_{cmax} , J_{max} , and foliar N, P and SLA developed from a global dataset (Walker *et al.*, 2014). Walker’s minimum adequate model (Model 1, Table 3 in Walker *et al.*, 2014) predicts V_{cmax} from values of N_{area} and P_{area} , including a term for their interaction, based on 110 observations of both tropical and temperate species measured in both the field and the laboratory. J_{max} was predicted solely as a function of V_{cmax} (Model 4 in Table 3, Walker *et al.*, 2014). Using our measured values of N_{area}

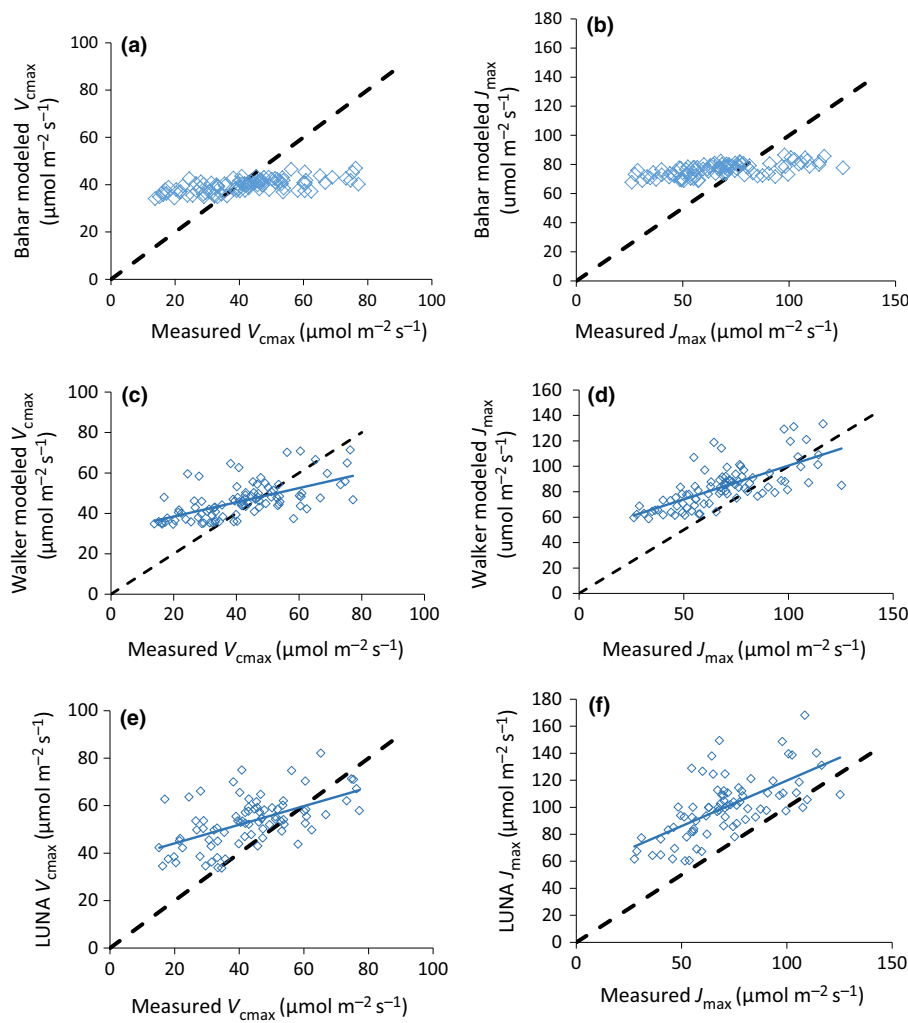


Fig. 6 Comparison of observed values of (a, c, e) maximal Rubisco carboxylation rate (V_{cmax}) and (b, d, f) maximum electron transport rate (J_{max}), standardized to 25°C, and predictions from the empirical relationships described by (a, b) Bahar *et al.* (2016) and (c, d) Walker *et al.* (2014), and (e, f) modeled mechanistically with the LUNA model (Ali *et al.*, 2016; Xu *et al.*, 2012). Dotted lines indicate a 1 : 1 relationship. See Table 3 for statistics of reduced major axis regressions.

and P_{area} , both V_{cmax} and J_{max} were overpredicted at low values (Fig. 6c,d). The modeled means of V_{cmax} and J_{max} were 10% and 22% higher than the measured values, respectively. We also compared our field data to predictions from a mechanistic model of photosynthetic capacity, the LUNA model (Leaf Utilization of Nitrogen for Assimilation; Xu *et al.*, 2012; Ali *et al.*, 2016). LUNA predicts photosynthetic capacity mechanistically by maximizing net photosynthetic carbon gain, given N_{mass} , leaf mass per area (LMA) and empirical N use strategies under different climate conditions, including radiation, temperature, humidity and day length. We challenged the LUNA model to predict V_{cmax} and J_{max} for the trees in our dataset using only the measured N_{mass} , LMA, and the time and location of sampling. We used the default parameter values estimated by fitting the LUNA model to a global dataset of V_{cmax} and J_{max} (Ali *et al.*, 2015, 2016). The modeled values of V_{cmax} and J_{max} based on this mechanistic approach showed similar deviations from measured values to the empirically derived predictions based on Walker *et al.* (2014) (Fig. 6e,f). Whether these deviations indicate a temperate forest bias in model parameterization or insufficient model sensitivity that flattens the model vs data slope is unclear, but model predictions may be improved with further observations of tropical trees.

Our analyses do not support the expectation that for trees growing on lowland tropical soils, the $V_{\text{cmax}}\text{-P}$ relationship should be stronger than the $V_{\text{cmax}}\text{-N}$ relationship (Domingues *et al.*, 2010), given that relationships based only on P content were of similar strength to those based on N content. However, we note that the foliar nutrient concentrations we observed, especially at the relatively fertile PNM site, tended to be greater than those observed in other tropical forests. Our data do support the expectation that the relationship between J_{max} and P should be stronger than the relationship between V_{cmax} and P (Domingues *et al.*, 2010), and multivariate regression indicated that the best fit for the data came from the predictions based on both P_{area} and N_{area} , in agreement with the minimum adequate model of Walker *et al.* (2014). Is there value in including P_{area} as a predictor? Doing so will be possible only if values of foliar P content can be generated from routines based on soil P availability or set as an input variable for a given PFT. Either approach will inevitably introduce increased complexity and uncertainty. The LUNA model does not currently include any influence of P and there is not a compelling mechanistic basis for doing so. An approach for incorporating P could be to derive separate relationships for V_{cmax} vs N_{area} for low, medium and high values of P_{area} ,

similar to the approach of Reich *et al.* (2009). However, the significant relationship between V_{cmax} and N_{area} in Fig. 5(b) broke down when the dataset was segmented by foliar P (Fig. S3). Bahar *et al.* (2016) also saw no significant effect of P_{area} on V_{cmax} per unit N, and they concluded that soil or leaf P is unlikely to be a useful predictor of Rubisco capacity per unit leaf N. Photosynthetic N use efficiency (NUE) declined in glasshouse-grown tropical trees under P-limited conditions (Bloomfield *et al.*, 2014), but we saw no effect of P_{area} on NUE. Despite these limitations, including P content as a predictor should remain a research objective because including P will increase the confidence in predictions from ecosystem models under future conditions, such as elevated atmospheric CO₂, which could alter the availability of P in P-limited ecosystems (Cernusak *et al.*, 2011, 2013; Yang *et al.*, 2014; Norby *et al.*, 2016), or across stages of forest development following disturbances that shift away from P limitation and toward N limitation in P-limited tropical forests (Herbert *et al.*, 2003; Davidson *et al.*, 2007).

Conclusions

This survey of >100 tropical woody plants of diverse species from two sites in Panama differing in nutrient availability and plant community composition revealed a range in foliar nutrient concentrations and photosynthetic parameters. Trees at the more nutrient-depleted site (SLZ) had lower foliar N and P concentrations and contents than trees at the more fertile site (PNM), and the difference in P was larger, as reflected in the N:P ratio. The community composition of the two sites reflects adaptations to the different nutrient status: SLZ is dominated by species with affinity for low P, whereas PNM is dominated by species with affinity for high P (Condit *et al.*, 2013). With virtually no common species across sites in our dataset, the influence of species vs site cannot be disentangled. However, we saw no evidence of a species or phylogenetic effect, and the relationships between foliar nutrients and photosynthetic parameters did not differentiate between sites. Furthermore, in the several species for which there were multiple observations, variation in photosynthesis tracked the variation in nutrient content along the same relationship as developed for the entire mixed community. That is, points along these curves were more likely due to variation in edaphic conditions within or between sites, rather than to inherent difference among species.

The large variability observed among the many trees in this study might seem to create a formidable problem for modeling this ecosystem. However, our analysis shows that photosynthetic parameters could be predicted from relationships with foliar nutrient content that are robust across species and site. We see no basis from this analysis for subdividing the broadleaf tropical evergreen PFT into distinct groups with different parameter values, despite the wide variation in morphology and growth habit within this very diverse PFT. A better approach would be to capture the variability in photosynthetic parameters through their relationships with foliar nutrients. Although V_{cmax} and J_{max} could be adequately predicted based on N content, as is already included in some models, the predictions were improved

somewhat with the inclusion of P content. Including P could be especially important for predictions into future conditions. Driving variation in photosynthesis through foliar nutrient status, however, will be useful only if there are approaches for predicting nutrient content from edaphic conditions or other environmental drivers. Hence, close integration of the model–data connection in belowground and aboveground processes is needed. We also observed an improvement in predictive relationships when wood density was included, suggesting that trait covariance may be a useful approach for improving physiological expressions of photosynthesis in nutrient-enabled models.

Acknowledgements

We are grateful to Jorge Aranda of the Smithsonian Tropical Research Institute for invaluable assistance with species identification. We also thank Tomas Domingues for providing R script and Joe Wright for sharing leaf trait data. Stan Wullschleger, Xiaojuan Yang and three anonymous reviewers provided helpful comments on an earlier draft. Research sponsored by the Laboratory Directed Research and Development Program of Oak Ridge National Laboratory, managed by UT-Battelle, LLC, for the US Department of Energy under contract number DE-AC05-00OR22725. This research was also supported as part of the Next Generation Ecosystem Experiments-Tropics, funded by the US Department of Energy, Office of Science, Office of Biological and Environmental Research.

Author contributions

R.J.N. collected and analyzed the data and wrote the manuscript; L.G. designed the research, collected and analyzed the data and contributed to the manuscript; I.C.H. organized and analyzed the data; A.M.J., J.M.W. and D.J.W. collected the data; B.L.T. ran the nutrient analysis and contributed to the manuscript; A.P.W. collected and analyzed the data and contributed to the manuscript; C.X. analyzed the data and contributed to the manuscript; and K.W. designed the research, assisted in the field and contributed to the manuscript.

References

- Ali AA, Xu C, Rogers A, Fisher RA, Wullschleger SD, Massoud EC, Vrugt JA, Muss JD, McDowell NG, Fisher JB *et al.* 2016. A global scale mechanistic model of photosynthetic capacity (LUNA V1.0). *Geoscientific Model Development* 9: 587–606.
- Ali AA, Xu CG, Rogers A, McDowell NG, Medlyn BE, Fisher RA, Wullschleger SD, Reich PB, Vrugt JA, Bauerle WL *et al.* 2015. Global-scale environmental control of plant photosynthetic capacity. *Ecological Applications* 25: 2349–2365.
- Bahar NHA, Ishida FY, Weerasinghe LK, Guerrieri R, O’Sullivan OS, Bloomfield KJ, Asner GP, Martin RE, Lloyd J, Malhi Y *et al.* 2016. Leaf-level photosynthetic capacity in lowland Amazonian and high-elevation Andean tropical moist forests of Peru. *New Phytologist*. doi: 10.1111/nph.14079.
- Bloomfield KJ, Farquhar GD, Lloyd J. 2014. Photosynthesis-nitrogen relationships in tropical forest tree species as affected by soil phosphorus availability: a controlled environment study. *Functional Plant Biology* 41: 820–832.

- Bohonak AJ.** 2004. *RMA: Software for reduced major axis regression*. [WWW document] URL <http://www.bio.sdsu.edu/pub/andy/RMA.html> [accessed 11 September 2016].
- von Caemmerer S.** 2000. *Biochemical models of leaf photosynthesis*. *Techniques in plant sciences No 2*. Collingwood, Australia: CSIRO Publishing.
- Carswell FE, Grace J, Lucas ME, Jarvis PG.** 2000. Interaction of nutrient limitation and elevated CO₂ concentration on carbon assimilation of a tropical tree seedling (*Cedrela odorata*). *Tree Physiology* 20: 977–986.
- Cernusak LA, Winter K, Dalling JW, Holtum JAM, Jaramillo C, Körner C, Leakey ADB, Norby RJ, Poulter B, Turner BL et al.** 2013. Tropical forest responses to increasing atmospheric CO₂: current knowledge and opportunities for future research. *Functional Plant Biology* 40: 531–551.
- Cernusak LA, Winter K, Turner BL.** 2011. Transpiration modulates phosphorus acquisition in tropical tree seedlings. *Tree Physiology* 31: 878–885.
- Chave J, Coomes D, Jansen S, Lewis SL, Swenson NG, Zanne AE.** 2009. Towards a worldwide wood economics spectrum. *Ecology Letters* 12: 351–366.
- Chave J, Muller-Landau HC, Baker TR, Easdale TA, ter Steege H, Webb CO.** 2006. Regional and phylogenetic variation of wood density across 2456 neotropical tree species. *Ecological Applications* 16: 2356–2367.
- Condit R, Engelbrecht BMJ, Pino D, Perez R, Turner BL.** 2013. Species distributions in response to individual soil nutrients and seasonal drought across a community of tropical trees. *Proceedings of the National Academy of Sciences, USA* 110: 5064–5068.
- Davidson EA, de Carvalho CJR, Figueira AM, Ishida FY, Ometto JPHB, Nardoto GB, Sabá RT, Hayashi SN, Leal EC, Vieira ICG et al.** 2007. Recuperation of nitrogen cycling in Amazonian forests following agricultural abandonment. *Nature* 447: 995–998.
- Díaz-Espejo A, Walcroft AS, Fernandez JE, Hafidi B, Palomo MJ, Giron IF.** 2006. Modeling photosynthesis in olive leaves under drought conditions. *Tree Physiology* 26: 1445–1456.
- Dietze MC.** 2014. Gaps in knowledge and data driving uncertainty in models of photosynthesis. *Photosynthesis Research* 119: 3–14.
- Domingues TF, Ishida FY, Feldpausch TR, Grace J, Meir P, Saiz G, Sene O, Schrodt F, Sonke B, Taedoumg H et al.** 2015. Biome-specific effects of nitrogen and phosphorus on the photosynthetic characteristics of trees at a forest-savanna boundary in Cameroon. *Oecologia* 178: 659–672.
- Domingues TF, Martinelli LA, Ehleringer JR.** 2007. Ecophysiological traits of plant functional groups in forest and pasture ecosystems from eastern Amazonia, Brazil. *Plant Ecology* 193: 101–112.
- Domingues TF, Meir P, Feldpausch TR, Saiz G, Veenendaal EM, Schrodt F, Bird M, Djagbletey G, Hien F, Compaore H et al.** 2010. Co-limitation of photosynthetic capacity by nitrogen and phosphorus in West Africa woodlands. *Plant, Cell & Environment* 33: 959–980.
- Ellsworth DS, Crous KY, Lambers H, Cooke J.** 2015. Phosphorus recycling in photorespiration maintains high photosynthetic capacity in woody species. *Plant, Cell & Environment* 38: 1142–1156.
- Farquhar GD, Caemmerer SV, Berry JA.** 1980. A biochemical-model of photosynthetic CO₂ assimilation in leaves of C₃ species. *Planta* 149: 78–90.
- Fyllas NM, Patino S, Baker TR, Nardoto GB, Martinelli LA, Quesada CA, Paiva R, Schwarz M, Horna V, Mercado LM et al.** 2009. Basin-wide variations in foliar properties of Amazonian forest: phylogeny, soils and climate. *Biogeosciences* 6: 2677–2708.
- Garrison V, Cernusak LA, Winter K, Turner BL.** 2010. Nitrogen to phosphorus ratio of plant biomass versus soil solution in a tropical pioneer tree, *Ficus insipida*. *Journal of Experimental Botany* 61: 3735–3748.
- Goll DS, Brovkin V, Parida BR, Reick CH, Kattge J, Reich PB, van Bodegom PM, Niinemets U.** 2012. Nutrient limitation reduces land carbon uptake in simulations with a model of combined carbon, nitrogen and phosphorus cycling. *Biogeosciences* 9: 3547–3569.
- Gu L, Norby RJ, Haworth IC, Jensen AM, Turner BL, Walker AP, Warren JM, Weston DJ, Winter K.** 2016. *Photosynthetic parameters and nutrient content of trees at the Panama crane sites*. Oak Ridge, Tennessee, USA: Next Generation Ecosystem Experiments Tropics Data Collection, Carbon Dioxide Information Analysis Center, Oak Ridge National Laboratory [WWW document] URL <http://dx.doi.org/10.15486/NGT/1255260> [accessed 11 September 2016].
- Gu LH, Pallardy SG, Tu K, Law BE, Wullschleger SD.** 2010. Reliable estimation of biochemical parameters from C₃ leaf photosynthesis-intercellular carbon dioxide response curves. *Plant, Cell & Environment* 33: 1852–1874.
- Güsewell S.** 2004. N : P ratios in terrestrial plants: variation and functional significance. *New Phytologist* 164: 243–266.
- Hättenschwiler S, Aeschlimann B, Couteaux M-M, Roy J, Bonal D.** 2008. High variation in foliage and leaf litter chemistry among 45 tree species of a neotropical rainforest community. *New Phytologist* 179: 165–175.
- Hedin LO, Vitousek PM, Matson PA.** 2003. Nutrient losses over four million years of tropical forest development. *Ecology* 84: 2231–2255.
- Herbert DA, Williams M, Rastetter EB.** 2003. A model analysis of N and P limitation on carbon accumulation in Amazonian secondary forest after alternate land-use abandonment. *Biogeochemistry* 65: 121–150.
- Hietz P, Rosner S, Hietz-Seifert U, Wright SJ.** 2016. Wood traits related to size and life history of trees in a Panamanian rainforest. *New Phytologist*. doi:10.1111/nph.14123.
- Karla YP, ed.** 1998. *Handbook of reference methods for plant analysis*. Boca Raton, FL, USA: CRC Press.
- Kattge J, Knorr W, Raddatz T, Wirth C.** 2009. Quantifying photosynthetic capacity and its relationship to leaf nitrogen content for global-scale terrestrial biosphere models. *Global Change Biology* 15: 976–991.
- Kenzo T, Ichie T, Watanabe Y, Yoneda R, Ninomiya I, Koike T.** 2006. Changes in photosynthesis and leaf characteristics with tree height in five dipterocarp species in a tropical rain forest. *Tree Physiology* 26: 865–873.
- Lambers H, Raven JA, Shaver GR, Smith SE.** 2008. Plant nutrient-acquisition strategies change with soil age. *Trends in Ecology & Evolution* 23: 95–103.
- Long SP, Bernacchi CJ.** 2003. Gas exchange measurements, what can they tell us about the underlying limitations to photosynthesis? Procedures and sources of error. *Journal of Experimental Botany* 54: 2393–2401.
- Long SP, Farage PK, Garcia RL.** 1996. Measurement of leaf and canopy photosynthetic CO₂ exchange in the field. *Journal of Experimental Botany* 47: 1629–1642.
- Luo YQ, Melillo J, Niu SL, Beier C, Clark JS, Classen AT, Davidson E, Dukes JS, Evans RD, Field CB et al.** 2011. Coordinated approaches to quantify long-term ecosystem dynamics in response to global change. *Global Change Biology* 17: 843–854.
- Medlyn BE, Dreyer E, Ellsworth D, Forstreuter M, Harley PC, Kirschbaum MUF, Le Roux X, Montpiet P, Strassmeyer J, Walcroft A et al.** 2002. Temperature response of parameters of a biochemically based model of photosynthesis. II. A review of experimental data. *Plant, Cell & Environment* 25: 1167–1179.
- Medlyn BE, Zaehle S, De Kauwe MG, Walker AP, Dietze MC, Hanson PJ, Hickler T, Jain AK, Luo Y, Parton W et al.** 2015. Using ecosystem experiments to improve vegetation models. *Nature Climate Change* 5: 528–534.
- Meir P, Levy PE, Grace J, Jarvis PG.** 2007. Photosynthetic parameters from two contrasting woody vegetation types in West Africa. *Plant Ecology* 192: 277–287.
- Mercado LM, Patino S, Domingues TF, Fyllas NM, Weedon GP, Sitch S, Quesada CA, Phillips OL, Aragao LEOC, Malhi Y et al.** 2011. Variations in Amazon forest productivity correlated with foliar nutrients and modelled rates of photosynthetic carbon supply. *Philosophical Transactions of the Royal Society B* 366: 3316–3329.
- Nascimento HEM, Laurance WF, Condit R, Laurance SG, D'Angelo S, Andrade AC.** 2005. Demographic and life-history correlates for Amazonian trees. *Journal of Vegetation Science* 16: 625–634.
- Norby RJ, De Kauwe MG, Domingues TF, Duursma RA, Ellsworth DS, Goll DS, Lapola DM, Luus KA, MacKenzie AR, Medlyn BE et al.** 2016. Model-data synthesis for the next generation of forest free-air CO₂ enrichment (FACE) experiments. *New Phytologist* 209: 17–28.
- Oleson KW, Lawrence DM (coordinating lead authors).** 2013. *Technical description of version 4.5 of the Community Land Model (CLM) NCAR/TN-503 + STR*. Boulder, CO, USA: National Center for Atmospheric Research.
- Patino S, Lloyd J, Paiva R, Baker TR, Quesada CA, Mercado LM, Schmerler J, Schwarz M, Santos AJB, Aguilar A et al.** 2009. Branch xylem density variations across the Amazon Basin. *Biogeosciences* 6: 545–568.

- Quesada CA, Phillips OL, Schwarz M, Czimczik CI, Baker TR, Patino S, Fyllas NM, Hodnett MG, Herrera R, Almeida S *et al.* 2012. Basin-wide variations in Amazon forest structure and function are mediated by both soils and climate. *Biogeosciences* 9: 2203–2246.
- R Core Development Team. 2011. *R: a language and environment for statistical computing*. Vienna, Austria: R Foundation for Statistical Computing.
- Rao IM. 1997. The role of phosphorus in photosynthesis. In: Pessarakli M, ed. *Handbook of photosynthesis*. New York, USA: Marcel Dekker Inc., 173–194.
- Reed SC, Yang X, Thornton PE. 2015. Incorporating phosphorus cycling into global modeling efforts: a worthwhile, tractable endeavor. *New Phytologist* 208: 324–329.
- Reich PB, Oleksyn J. 2004. Global patterns of plant leaf N and P in relation to temperature and latitude. *Proceedings of the National Academy of Sciences, USA* 101: 11001–11006.
- Reich PB, Oleksyn J, Wright IJ. 2009. Leaf phosphorus influences the photosynthesis-nitrogen relation: a cross-biome analysis of 314 species. *Oecologia* 160: 207–212.
- Rogers A. 2014. The use and misuse of $V_{c,\max}$ in Earth System Models. *Photosynthesis Research* 119: 15–29.
- Rowland L, Lobo-do-Vale RL, Christoffersen BO, Melem EA, Krujft B, Vasconcelos SS, Domingues T, Binks OJ, Oliveira AAR, Metcalfe D *et al.* 2015. After more than a decade of soil moisture deficit, tropical rainforest trees maintain photosynthetic capacity, despite increased leaf respiration. *Global Change Biology* 21: 4662–4672.
- Santiago LS, Schuur EAG, Silvera K. 2005. Nutrient cycling and plant-soil feedbacks along a precipitation gradient in lowland Panama. *Journal of Tropical Ecology* 21: 461–470.
- Schimel D, Stephens BB, Fisher JB. 2015. Effect of increasing CO₂ on the terrestrial carbon cycle. *Proceedings of the National Academy of Sciences, USA* 112: 436–441.
- Sharkey TD, Bernacchi CJ, Farquhar GD, Singsaas EL. 2007. Fitting photosynthetic carbon dioxide response curves for C₃ leaves. *Plant, Cell & Environment* 30: 1035–1040.
- Sivak MN, Walker AD. 1986. Photosynthesis *in vivo* can be limited by phosphate supply. *New Phytologist* 102: 499–512.
- Smith RJ. 2009. Use and misuse of the reduced major axis for line-fitting. *American Journal of Physical Anthropology* 140: 476–486.
- Thomas RQ, Brookshire ENJ, Gerber S. 2015. Nitrogen limitation on land: how can it occur in Earth system models? *Global Change Biology* 21: 1777–1793.
- Townsend AR, Cleveland CC, Asner GP, Bustamante MMC. 2007. Controls over foliar N : P ratios in tropical rain forests. *Ecology* 88: 107–118.
- Turner BL, Romero TE. 2009. Short-term changes in extractable inorganic nutrients during storage of tropical rain forest soils. *Soil Science Society of America Journal* 73: 1972–1979.
- Vitousek PM, Sanford RL. 1986. Nutrient cycling in moist tropical forest. *Annual Review of Ecology and Systematics* 17: 137–167.
- Walker AP, Beckerman AP, Gu LH, Kattge J, Cernusak LA, Domingues TF, Scales JC, Wohlfahrt G, Wullschleger SD, Woodward FI. 2014. The relationship of leaf photosynthetic traits – $V_{c,\max}$ and J_{\max} – to leaf nitrogen, leaf phosphorus, and specific leaf area: a meta-analysis and modeling study. *Ecology and Evolution* 4: 3218–3235.
- Wang YP, Law RM, Pak B. 2010. A global model of carbon, nitrogen and phosphorus cycles for the terrestrial biosphere. *Biogeosciences* 7: 2261–2282.
- Wright SJ, Kitajima K, Kraft NJB, Reich PB, Wright IJ, Bunker DE, Condit R, Dalling JW, Davies SJ, Diaz S *et al.* 2010. Functional traits and the growth-mortality trade-off in tropical trees. *Ecology* 91: 3664–3674.
- Wullschleger SD. 1993. Biochemical limitations to carbon assimilation in C₃ plants – a retrospective analysis of the A/Ci curves from 109 species. *Journal of Experimental Botany* 44: 907–920.
- Wullschleger SD, Epstein HE, Box EO, Euskirchen ES, Goswami S, Iversen CM, Kattge J, Norby RJ, van Bodegom PM, Xu XF. 2014. Plant functional types in Earth system models: past experiences and future directions for application of dynamic vegetation models in high-latitude ecosystems. *Annals of Botany* 114: 1–16.
- Xu CG, Fisher R, Wullschleger SD, Wilson CJ, Cai M, McDowell NG. 2012. Toward a mechanistic modeling of nitrogen limitation on vegetation dynamics. *PLoS ONE* 7: e37914.
- Yang X, Post WM, Thornton PE, Jain A. 2013. The distribution of soil phosphorus for global biogeochemical modeling. *Biogeosciences* 10: 2525–2537.
- Yang X, Thornton PE, Ricciuto DM, Post WM. 2014. The role of phosphorus dynamics in tropical forests – a modeling study using CLM-CNP. *Biogeosciences* 11: 1667–1681.
- Zanne AE, Lopez-Gonzalez G, Coomes DA, Ilic J, Jansen S, Lewis SL, Miller RB, Swenson NG, Wiemann MC, Chave J. 2009. Data from: Towards a worldwide wood economics spectrum. *Dryad Digital Repository*. <http://dx.doi.org/10.5061/dryad.234>.

Supporting Information

Additional Supporting Information may be found online in the Supporting Information tab for this article:

Fig. S1 The relationship between J_{\max} and P_{area} , as presented in Fig. 5(c), highlighting four species for which there were multiple observations.

Fig. S2 Measurements of $V_{c,\max}$ and J_{\max} of lowland and upland species in tropical moist forests of Peru from Bahar *et al.* (2016) compared with values predicted from bivariate relationships with P_{area} developed in this study.

Fig. S3 $V_{c,\max}$ vs N_{area} , as in Fig. 5(b), segmented by low, medium and high P_{area} .

Table S1 Plant species (trees, lianas and perennial herbs) in the final dataset

Please note: Wiley Blackwell are not responsible for the content or functionality of any Supporting Information supplied by the authors. Any queries (other than missing material) should be directed to the *New Phytologist* Central Office.